Computers in Biology and Medicine 196 (2025) 110908

Contents lists available at ScienceDirect

Computers in Biology and Medicine

journal homepage: www.elsevier.com/locate/compbiomed

Video-based markerless assessment of bilateral upper limb motor activity following cervical spinal cord injury

Beatrice Lagomarsino [a,b], Antonino Massone [c], Francesca Odone [a,d], Maura Casadio [a,1], Matteo Moro [a,d,*,1]

[a] Department of Informatics, Bioengineering, Robotics and Systems Engineering (DIBRIS), University of Genova, Genova, Italy
[b] Movendo Technology s.r.l., Genova, Italy
[c] Spinal Cord Unit, Santa Corona Hospital, ASL2 Savonese, Pietra Ligure, Italy
[d] Machine Learning Genoa (MaLGa) Center, Genova, Italy

ARTICLE INFO

Keywords:
Markerless human motion analysis
Spinal cord injury
Video analysis
MediaPipe
Alphapose

ABSTRACT

Background: Recent advancements in computer vision have positioned pose estimation as a powerful tool for analyzing human movement from video data. However, its application to neurological populations, particularly individuals with spinal cord injuries (SCI), remains largely unexplored.
Objective: To evaluate the effectiveness of three video-based pose estimation algorithms in detecting upper limb motor impairments in individuals with cervical SCI, and to determine their reliability and sensitivity in comparison with marker-based motion capture.
Methods: Twelve individuals with cervical SCI and twelve unimpaired controls performed four static arm poses from the Arm Stabilization Test (part of the Van Lieshout Arm/Hand Function Test). Three pose estimation methods — MediaPipe 2D, AlphaPose, and MediaPipe 3D — were applied to single-camera videos, and results were compared to kinematics captured by an eight-camera marker-based motion capture system. Motor performance was quantified using a compensation ratio (shoulder vs. elbow movement), and trial-by-trial repeatability was assessed.
Results: All three algorithms demonstrated strong repeatability. MediaPipe 3D, in particular, showed a significant correlation between the compensation metric and impairment severity, effectively distinguishing SCI from control participants. In contrast, 2D methods lacked this sensitivity, likely due to the absence of depth information.
Conclusion: Markerless pose estimation, especially 3D approaches, offers a promising, non-invasive alternative for assessing upper limb motor function in neurological populations. These tools could expand accessibility to motor assessment in both clinical and research settings, although further research is needed to assess their sensitivity to subtle impairments.

1. Introduction

Kinematic analysis has the potential to support the understanding and assessment of motor functions in clinics. This is particularly important in individuals with cervical spinal cord injury (cSCI) [1–5]. These injuries often result in partial or complete loss of motor and sensory functions below the injury site, leading to bilateral upper limb impairments [6,7]. This can severely impact the ability to perform daily activities. Precise evaluation of upper limb function is crucial for developing effective rehabilitation strategies [3]. By analyzing and quantifying movement, clinicians can identify specific impairments, track progress, and guide interventions, making kinematic assessment a powerful tool in the treatment of cSCI.

Traditional kinematic analysis techniques often involve infrared marker-based motion capture systems [3]. These systems provide precise and accurate measurements in three-dimensional (3D) space and are used for quantitative assessments of neuromotor functions during movement in various neurological diseases, such as stroke and multiple sclerosis [1,2,8,9]. However, marker-based systems come with several limitations [10]. They are expensive, require complex and time-consuming setup procedures, and may affect the naturalness of

* Corresponding author at: Department of Informatics, Bioengineering, Robotics and Systems Engineering (DIBRIS), University of Genova, Genova, Italy.
E-mail address: matteo.moro@unige.it (M. Moro).
[1] M. Casadio and M. Moro share equal senior contribution.

https://doi.org/10.1016/j.compbiomed.2025.110908
Received 26 May 2025; Received in revised form 25 July 2025; Accepted 4 August 2025
Available online 16 August 2025

movement due to the need for placing markers on specific anatomical points [9]. Recent advancements in deep learning and computer vision have enabled the development of video-based markerless motion capture techniques. These techniques utilize video-based methods to analyze human motion without physical markers. Video-based markerless approaches offer several advantages over traditional marker-based systems [11]. They are non-invasive, cost-effective, and can be implemented using commonly available hardware such as smartphones and webcam data [12].

In this scenario, human pose estimation (HPE) algorithms [12,13] can be considered an alternative to marker-based approaches. Starting from video data, they detect the position of key body landmarks, allowing for quantitative human motion characterization. Among them, MediaPipe Pose [14–16] offers real-time performance even on smartphones, and AlphaPose [17] provides a good compromise between performance and accuracy compared with recent transformer-based algorithms that require more computational resources. Recently, several studies reported the great potential of HPE in the medical domain supporting clinicians in diagnosis [18,19], remote monitoring [20–22], rehabilitation tasks [20,23–25], and gait analysis [26,27] reducing the need for specialized equipment and saving significant healthcare resources [9,12,26,28]. In this context, HPE has gained increasing attention in telerehabilitation, where it enables real-time feedback and remote supervision of motor activities. These technologies allow people to perform therapeutic exercises at home while maintaining clinical oversight, thanks to their ability to operate efficiently on consumer devices such as smartphones and webcams, and to integrate seamlessly into mobile or web-based platforms. HPE has proven effective in remote rehabilitation settings, by supporting the assessment and continuous monitoring of motor performance. It enables accurate tracking of joint movements, detection of compensatory strategies, and supervision of therapeutic exercises, offering clinicians valuable insights into movement quality and patient adherence [29–34]. Furthermore, algorithms based on HPE may deliver automated, real-time feedback, helping patients correct their movements during unsupervised sessions and promoting greater engagement with home-based therapy [35–37]. This can be particularly beneficial in long-term rehabilitation programs, where consistency and motivation are often challenging to maintain [38]. By providing objective and quantifiable motion data without the need for specialized equipment, HPE contributes to a more accessible, scalable, and cost-effective model of care. This growing application underscores the potential of markerless pose estimation to improve access to care, ensure continuity of rehabilitation, and extend clinical services beyond traditional healthcare environments. Despite these promising developments, only a few studies are focusing on HPE applications in neurological populations [12,39–51], and mainly address gait analysis in conditions such as multiple sclerosis (MS), Parkinson's disease (PD), and stroke, with limited attention to upper limb assessment [52–55]. To our knowledge, only few studies have explored the use of HPE for assessing motor performance in individuals with SCI [56,57]. Although these works demonstrate the growing interest in markerless approaches for SCI, to date, no study has systematically compared multiple HPE algorithms, evaluated bilateral upper limb movements, or analyzed compensatory strategies in relation to lesion severity with video-based approaches.

The objective of this study is to fill these gaps by evaluating whether the three abovementioned video-based HPE methods (MediaPipe and Alphapose) can be used as a starting point to detect performance differences in motor tasks between cSCI and unimpaired people. To achieve this, we focused on a clinical function assessment involving coordinated bilateral movements required for the Stabilization sub-section of the "Van Lieshout arm/hand function test" (VLT) [58], and we analyzed the range of motion (ROM) and the normalized height between body joints starting from the acquisitions (both video- and marker-based) of 12 cSCI volunteers (C5-C7 lesions) and 12 age- and sex-matched unimpaired participants. For the video-based analysis, we employed two 2D pose estimation algorithms (MediaPipe and AlphaPose) and one 3D pose estimation algorithm (MediaPipe Pose 3D). To assess their effectiveness, we compare the identified differences with those observed using a gold standard motion capture system, recorded simultaneously. Given the importance of measurement repeatability, we also examine the consistency across trials of the kinematic parameters obtained with the markerless techniques. Ensuring robust and reproducible results is crucial for the application of markerless approaches in both clinical and research contexts. We expect the proposed assessment will offer clinicians a reliable, comprehensive, and easy-to-use method for evaluating bilateral neuromotor deficits after a cervical injury.

1.1. Statement of significance

(1) **Problem or issue.** Evaluating upper limb function in individuals with cervical spinal cord injury (SCI) is essential but limited by the cost and complexity of traditional motion capture systems. Markerless pose estimation offers a potential solution, yet its application in this context remains underexplored.
(2) **What is already known.** Marker-based systems are the standard for precise kinematic assessment, and markerless pose estimation has shown promise in various clinical applications. However, research on its use for upper limb assessment in SCI populations is limited.
(3) **What this paper adds.** This study is one of the first attempts to assess markerless pose estimation methods for detecting motor impairments in people with SCI, demonstrating their reliability and ability to capture compensatory strategies.
(4) **Who would benefit from the new knowledge in this paper.** Clinicians, researchers, and medical technology developers will benefit from these findings, which support the use and highlight the limitations of accessible, non-invasive tools for evaluating upper limb function in neurological populations.

2. Materials and methods

2.1. Experimental setup and protocol

Twelve people with cervical spinal lesions (age 34.7 ± 13.5 years, 4 females; lesion level between C5 and C7: with 2 C7, 5 C6, and 5 C5) and twelve age- and sex-matched unimpaired volunteers (age 34.7 ± 13.5 years, 4 females) participated in the study. The sample size was determined based on feasibility considerations and previous studies involving individuals with cervical SCI, a population that is inherently limited in size and more difficult to recruit than other neurological cohorts. During the recruitment period, all eligible people with SCI from the regional rehabilitation center who met the inclusion criteria were enrolled. The resulting sample size (12 SCI participants and 12 controls) is comparable to that reported in prior work using video-based motion analysis in similar clinical populations [9,56,57]. The data were acquired at the Spinal Cord Unit of the Santa Corona Hospital in Pietra Ligure (Italy) following the national guidelines and the ethical standards of the Declaration of Helsinki (2013 revision) and the retrospective study was approved by the local ethical review board (Comitato Etico Regione Liguria, protocol n. CER Liguria: 585/2021). The inclusion criteria for SCI individuals were a cervical spinal cord injury between C5 and C7 (complete lesion American Spinal Injury Association (ASIA) grade A or incomplete lesion ASIA grade B or C) and the ability to perform shoulder and arm movements. All participants signed informed consent, which included consent to the data analysis for scientific purposes and the publication of the results. All the participants performed 4 poses of the arm stabilization task from the "Van Lieshout arm/hand function test" (VLT) manual, typically used to assess bilateral arm movement coordination. The VLT manual is clinically used to evaluate arm and hand function with tasks representing the level of activity outlined in the International Classification

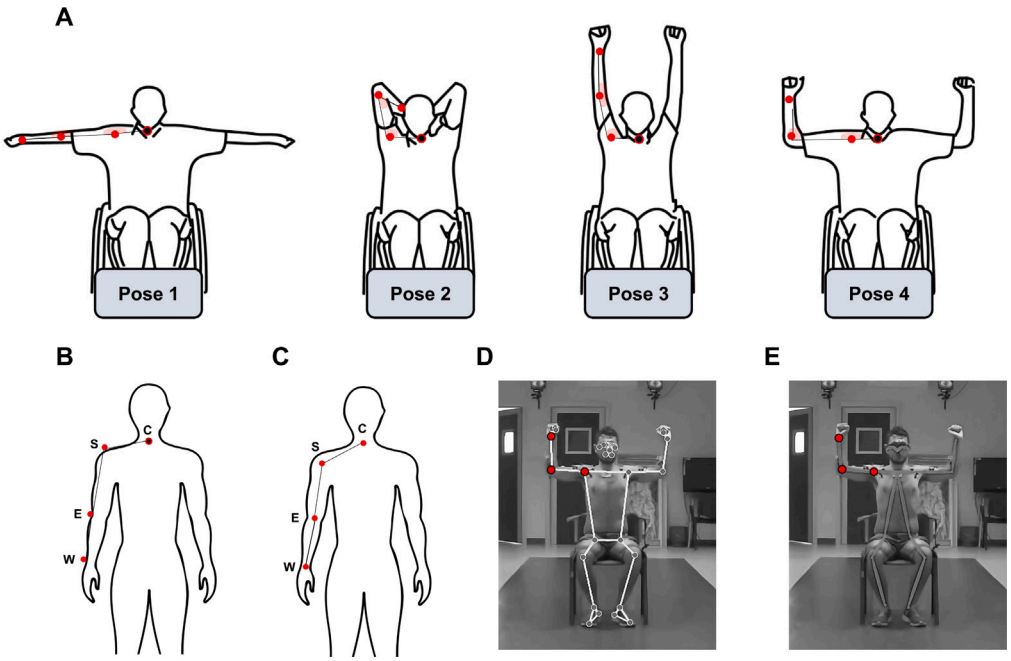

Fig. 1. (A) The selected four poses of the arm stabilization task of the VLT manual, the red shades are a sketch of elbow and shoulder angles computed for each pose; (B) physical marker placement: C is C7, S is the shoulder, E is the elbow, and W the wrist; C) Pose estimators keypoints' placement: C is the middle point between the shoulders, S is the shoulder, E the elbow and W the wrist. (D) Red dots are the selected keypoints detected with MediaPipe and (E) with AlphaPose.

of Functioning, Disability, and Health [58]. Our assessment utilized the task designed to evaluate bilateral arm function. This task requires participants to maintain specific poses stabilizing both arms in space against gravity for 5 s. We focused on four different poses of increasing difficulty, with the first pose (Pose 1) being identified as the least demanding movement. Participants were instructed to assume each pose at their preferred speed. Detail descriptions of each pose (Fig. 1A) are as follows: in Pose 1, the arms are placed horizontally (parallel to the floor) in a lateral direction, with the elbows fully extended and the thumbs pointing posteriorly; in Pose 2 the elbows point upward, completely flexed, with hands touching the neck and forearms against the head; in the Pose 3, the arms are positioned above the head with the elbows fully extended along the vertical axis and the upper arm rotating outward; in Pose 4 the arms are placed horizontally along the mediolateral axis, with the elbows flexed 90° in outward rotation. Note that the complete arm stabilization task includes five poses. However, we excluded the fifth pose because it differed from Pose 1 only by forearm pronation, which is challenging to distinguish using the selected markers (see next paragraph) and within the context of a 2D video analysis. The complete sequence of these four poses was repeated 6 times. The kinematic data were collected using a motion capture system (SMART DX, BTS Bioengineering, Milan, Italy) consisting of 8 infrared cameras (SMART-DX5000, BTS Bioengineering) and reflective spherical passive markers of 1.5 cm diameter. We recorded, at a sampling frequency of 100 Hz, the position of 7 markers positioned on the spinal process of C7 (C), and bilaterally on acromions (S), elbows (E), wrists (W) (Fig. 1B) [59]. During the acquisition, one video camera (BTS VIXTA, BTS Bioengineering) was positioned in front of the participants (frontal plane), recording their movements at 25 frames per second (frame dimensions: 640 × 480 pixels).

2.2. Kinematic data analysis

With the marker-based system, we obtained the markers' coordinates positioned on the participants' bodies (Fig. 1B). Using MediaPipe Pose 2D (version 0.10.14) and AlphaPose we extracted the positions of 3 keypoints in the image plane corresponding to a point on the shoulder, elbow, and wrist for both upper limbs (red dots in Fig. 1C). The same virtual maker positions were extracted in the 3D world coordinates (in meters) using MediaPipe Pose 3D (version 0.10.14). To address challenges posed by occlusions and mispredictions in tracking landmark positions from videos, we used the pose estimator's confidence score in landmarks detection to assess the reliability of detected points. Occluded landmarks were identified by low confidence values (lower than 0.7), while mispredictions manifested as abrupt spikes in landmark speeds. These artifacts were discarded, and short-term data gaps (less than 2 s) were reconstructed via pchip interpolation [60]. All the coordinates were low-pass filtered over time (Butterworth, 4th order, 12 Hz cut-off frequency) [61]. Confidence-based filtering was applied independently to the 2D and 3D outputs of MediaPipe, without transferring visibility or reliability information between them. The validation of 3D joint positions relied exclusively on the confidence scores provided by the MediaPipe 3D model (BlazePose GHUM). This method integrates 2D observations with additional information, including a statistical body model, temporal smoothing, and kinematic constraints, which enables it to infer plausible 3D joint positions even when certain keypoints are occluded in 2D [15,16]. To identify the time windows corresponding to pose maintenance, we analyzed the velocity profile of the wrist keypoint. Specifically, the correct time window was defined as an interval between two velocity peaks of opposite sign, corresponding to the forward and return movements. The starting point of the time window was identified as the last instant when the velocity dropped below 10% of the forward movement's peak velocity (positive peak). Similarly, the endpoint was determined as the last instant when the velocity was above 10% of the return movement's peak velocity (negative peak) [3]. To evaluate the ROM, we bilaterally computed the elbow and shoulder angles for each approach (*i.e.*, markerless and marker-based) by averaging the angle data obtained for all frames within each pose maintenance time window according to:

$$\theta_{A,B} = \cos^{-1}\left(\frac{\vec{A}\cdot\vec{B}}{|\vec{A}| * |\vec{B}|}\right) \quad (1)$$

where θ is the angle between two vectors A and B. We defined the segments as follows: *CS* represents the segment between points C (C7-middle point of shoulders) and S (shoulder), *SE* represents the segment between points S (shoulder) and E (elbow), and *EW* represents the

Table 1
Summary of the parameters considered in the study. The table reports the parameters extracted from both marker-based and markerless motion capture systems, including angles, normalized height between key body landmarks, and the shoulder-to-wrist ratio index. For each parameter, the table reports (if applicable) the label, a brief description, and the measurement units. The symbol "–" in the Units column indicates a dimensionless parameter.

Parameter	Label	Description	Units
Shoulder Angle	$\theta_{\vec{CS},\vec{SE}}$	Angle between upper arm and chest segment	Degrees (°)
Elbow Angle	$\theta_{\vec{SE},\vec{EW}}$	Angle between upper arm and forearm segments	Degrees (°)
Normalized Height Shoulder–Elbow	$nH_{S,E}$	Height of the elbow with respect to the shoulder, normalized by the shoulder–elbow distance	–
Normalized Height Elbow–Wrist	$nH_{E,W}$	Height of the wrist with respect to the elbow, normalized by the shoulder–elbow distance	–
Shoulder-to-Wrist Index	$R_{S,W}$	Ratio between shoulder and elbow angles	–

segment between points E (elbow) and W (wrist). According to Eq. (1), we calculated:

- **Shoulder Angle** ($\theta_{\vec{CS},\vec{SE}}$): the angle between the segments $\vec{CS}$ and $\vec{SE}$ (Fig. 1A).
- **Elbow Angle** ($\theta_{\vec{SE},\vec{EW}}$): the angle between the segments $\vec{SE}$ and $\vec{EW}$ (Fig. 1A).

We computed with the same approach the difference in height between shoulder and elbow and between elbow and wrist. We considered the relative positions of the keypoints and markers on the shoulder, elbow, and wrist during the pose maintenance, and, within each pose-maintenance time window, we computed the normalized Height (nH) *i.e.*, relative vertical position between a pair of body joints, normalized for the Euclidean distance between them [3] following the equation:

$$nH_{i,j} = \frac{|\, y_i - y_j \,|}{d(p_i - p_j)} \tag{2}$$

where y_i and y_j are the y-coordinates of points i and j, respectively, and $d(p_i, p_j)$ is the Euclidean distance between the positions of these two landmarks. As for the angles, the normalized height (nH) was computed bilaterally for the keypoints shoulder–elbow ($nH_{S,E}$) and elbow–wrist ($nH_{E,W}$). The calculation of both the angles and the normalized heights was performed in the image plane (*i.e.*, frontal plane) for the 2D pose estimation algorithms, and in the 3D reference systems for the 3D pose estimation algorithm and the stereophotogrammetric system. We also investigated whether differences in motor performance could be distinguished based on the level of spinal lesion (C5, C6, or C7). Specifically, we aimed to determine whether markerless motion capture techniques were capable of effectively identifying such differences. Our analysis focused on compensatory movements, with the goal of assessing whether the algorithm could detect movement patterns indicative of compensation in individuals with higher levels of impairment (*e.g.*, C5), who may reorganize their motor strategies to compensate for reduced elbow mobility. We examined potential compensatory strategies at the shoulder and elbow levels by computing the average ratio ($R_{S,W}$) between shoulder and elbow angles across the four different poses (p) for all methods.

$$R_{S,W} = \frac{1}{4}\sum_{p=1}^{4}\frac{\theta^{p}_{\vec{CS},\vec{SE}}}{\theta^{p}_{\vec{SE},\vec{EW}}} \tag{3}$$

We hypothesize that higher lesion levels are associated with reduced elbow extension capacity, leading to more pronounced proximal movements at the shoulder.

Table 1 provides an overview of all the kinematic parameters computed in this study using both marker-based and markerless motion capture systems.

2.3. Statistical analysis

We tested the hypothesis that markerless approaches can detect differences in movement performance between cSCI and the control populations and that these differences are the same detected by the marker-based system. We also verified that the results obtained from the marker-based and markerless approaches are repeatable across trials. Thus, we conducted a mixed-design ANOVA for each pose on the parameters 'angles' and 'normalized height '. The ANOVA had two within-subject factors, "arm" (dominant vs. non-dominant) and "repetition", and one between-subject factor, "population" (cSCI vs. control, Supplementary Table I). We analyzed each method independently to account for differences in the positioning of physical and virtual markers. Indeed, marker-based systems rely on the placement of physical markers, whereas markerless approaches estimate joint positions using pre-trained pose-estimation algorithms, detecting landmark points that are not coincident with the marker position (Fig. 1B and C) and, consequently, the calculated parameters, angles, and eights are expected to be different. Despite these differences, all the approaches estimate the same arm poses, and we expected the parameters computed with different methods to be correlated, leading to consistent results in distinguishing between the motor abilities of populations with varying motor abilities. A significant main effect of the population factor would support the notion that the cSCI group performs differently compared to the control group. We expect that when this effect is significant for the marker-based system it will be also significant for the markerless-based approaches, supporting our hypothesis. Furthermore, a non-significant repetition effect would indicate that the measurement method is generally repeatable, whereas a significant repetition ×population interaction would reflect differences in measurement repeatability across groups. Before each statistical analysis, parameters were tested with the Shapiro–Wilk test to verify the normality assumption (Supplementary Tables II and III), and Mauchly's test was performed to assess the sphericity assumption. The statistical analyses were performed within the Jamovi environment (Jamovi software 0.9.2.8, jamovi.org). Statistical significance was set at $p < 0.05$. In the figures, p-values smaller than 0.001 are denoted with "**", while p-values smaller than 0.05 are denoted with "*". A Bonferroni correction for multiple comparisons was applied to the ANOVA post hoc analysis. Furthermore, to investigate whether the $R_{S,W}$ ratio varied as a function of lesion level, Spearman's rank correlation coefficient was computed.

3. Results

3.1. Ability of pose estimation algorithms to differentiate motor activity between SCI and unimpaired populations

The markerless methods detected differences between the two populations, which were consistent with those detected by the marker-based

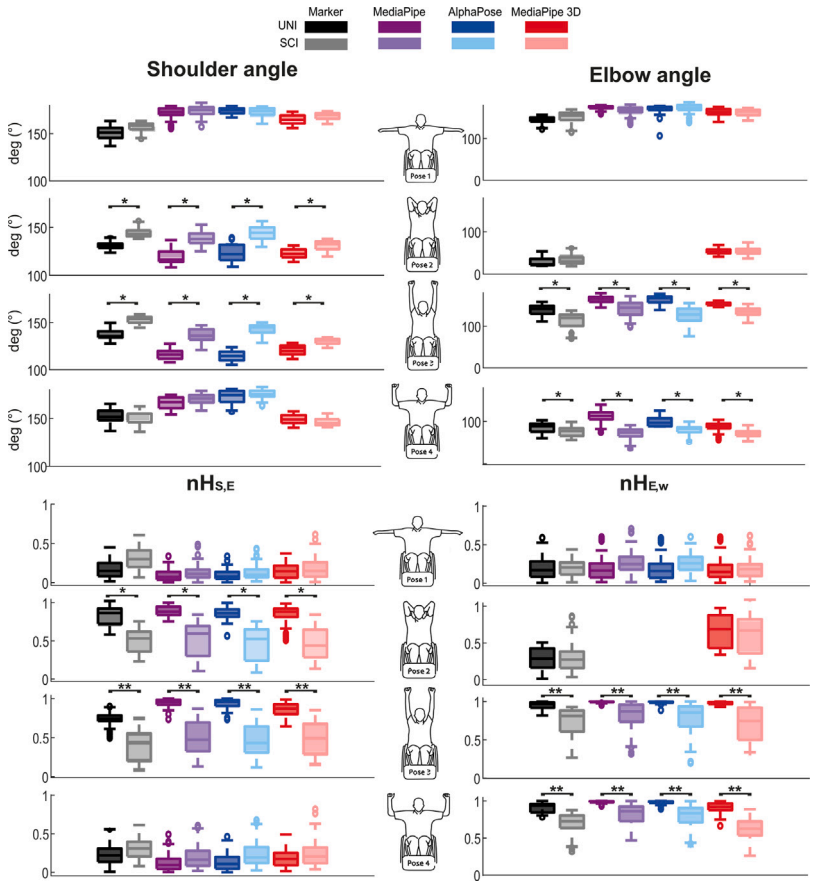

Fig. 2. Top: Shoulder (left) and elbow (right) angles for each pose. Bottom: Normalized Height (nH) values for each pose between shoulder and elbow ($nH_{S,E}$, left) and between elbow and wrist ($nH_{E,W}$, right). The boxplots represent the median and the 25th–75th percentiles of the data. Black, violet, blue, and red indicate values obtained using Marker-based system, MediaPipe, AlphaPose, and MediaPipe 3D, respectively, for the unimpaired (UNI) population. Gray, light violet, light blue, and rose indicate values obtained using Marker-based system, MediaPipe, AlphaPose, and MediaPipe 3D, respectively, for the spinal cord injury (SCI) population. In the figures, p-values smaller than 0.001 are denoted with "**", while p-values smaller than 0.05 are denoted with "*".

system for both the angles (Fig. 2 top) and the normalized heights (nH, Fig. 2 bottom). Detailed mean and standard deviation values for each parameter, across all poses and both populations, are reported in Supplementary Tables IV and V. Additionally, Supplementary Table I reports the statistical analysis results specifically for the population factor across all parameters and methods. Since the factor 'arm' (dominant vs. non-dominant) was not statistically significant for any method or pose (all $p > 0.4$), indicating no systematic asymmetries between limbs in either group, all reported outcomes were therefore averaged across arms.

In details: for Pose 1, both marker-based and markerless methods reported no statistical difference between the two populations for shoulder and elbow angles, $nH_{S,E}$ and $nH_{E,W}$.

Indeed, all participants demonstrate full extension of the arms horizontally and laterally, with symmetry between the two arms. For Pose 2, all methods found significant differences in shoulder angle and the $nH_{S,E}$ between the two populations. Indeed, cSCI participants tend not to fully flex the upper arm during the task, resulting in significantly lower values for the $nH_{S,E}$ parameter compared to control participants. Only two methods, MediaPipe 3D and the marker-based system, were able to estimate the elbow angle and the $nH_{E,W}$ because the position of the wrist in this pose was occluded in the frontal plane. Due to this occlusion, the 2D methods excluded the elbows and wrists from the analysis in Pose 2, as their confidence scores fell below the detection threshold. In contrast, MediaPipe 3D, supported by model-based inference, was able to reconstruct the posterior position of the upper limbs by interpreting the spatial configuration and orientation of keypoints in 3D space. This allowed for higher confidence scores and retention of those keypoints in the analysis. In this case, MediaPipe 3D and the marker-based system reported no statistical difference for both parameters. For Pose 3, all methods identified significant differences between the populations for shoulder and elbow angles as well as $nH_{S,E}$ and $nH_{E,W}$. Indeed, cSCI participants faced challenges in fully flexing shoulders and extending their elbows, evidenced by significantly lower values in the related parameters. For Pose 4 significant differences between the two populations in the elbow angle and $nH_{E,W}$ were consistent across methods, while no significant differences were detected for the shoulder angle and $nH_{S,E}$. Indeed, participants with cSCI were not able to maintain a flexion elbow angle of 90°.

3.2. Ability in highlighting motor differences between disability levels

We computed the shoulder-to-wrist index ($R_{S,W}$) for each method (*i.e.*, marker-based, MediaPipe 3D, MediaPipe 2D, and AlphaPose), and the results are presented in Fig. 3 and Table 2. The marker-based system revealed a increasing trend in the index: individuals with more severe impairments (*i.e.*, higher lesion levels such as C5) exhibited higher $R_{S,W}$ values, reflecting greater compensation through proximal joints. This trend was consistently captured by MediaPipe 3D (Fig. 3). Spearman correlation analysis supports these observations, indicating that both the marker-based system and MediaPipe 3D effectively captured a statistically significant and comparable correlation between the $R_{S,W}$ index and lesion level. Although MediaPipe 3D and the marker-based system showed strong correlation at the group level, some differences emerged at the individual level. In particular, the ranking of participants within the same lesion group was not always

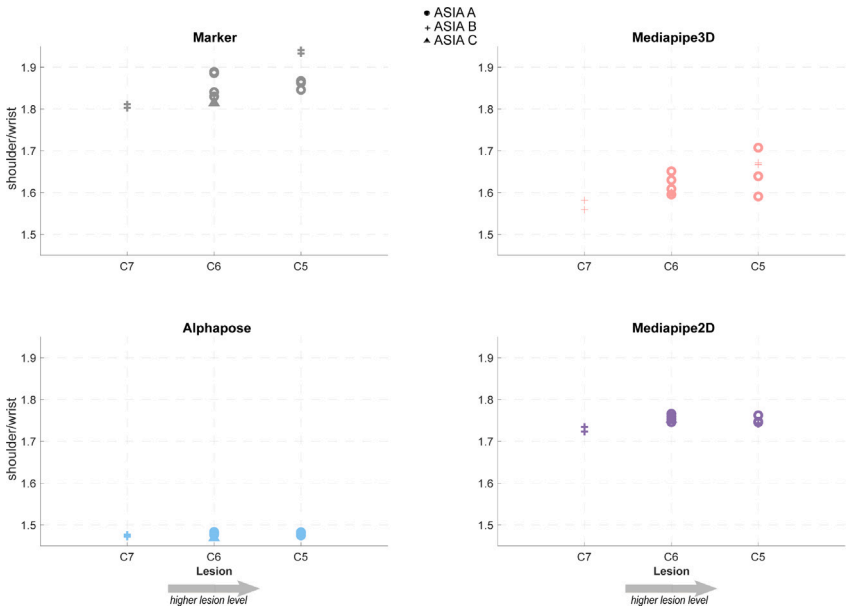

Fig. 3. $R_{S,W}$ index for each method (marker, MediaPipe3D, MediaPipe2D and Alphapose). Different marker shapes are used for different ASIA levels.

Table 2
$R_{S,W}$ index by lesion level (C5, C6, C7). We report the values for each method (mean and standard deviation across the participants for each group) and the results of the Spearman correlation coefficient.

Lesion level	Markers	MediaPipe 3D	MediaPipe 2D	Alphapose
C5	1.89 ± 0.04	1.66 ± 0.04	1.75 ± 0.07	1.48 ± 0.04
C6	1.85 ± 0.03	1.62 ± 0.02	1.76 ± 0.07	1.48 ± 0.05
C7	1.81 ± 0.04	1.57 ± 0.01	1.73 ± 0.06	1.47 ± 0.03
Rho/p-value	−0.70 / 0.01	−0.70 / 0.01	−0.17 / 0.60	−0.27 / 0.24

consistent between the two methods. In contrast, $R_{S,W}$ values obtained from the 2D methods (MediaPipe 2D and AlphaPose) appeared tightly clustered, showing no evident progression across lesion levels. This compressed distribution likely limits their ability to detect consistent compensation strategies related to injury severity. Accordingly, the correlations between $R_{S,W}$ and lesion level for the 2D methods were not statistically significant.

For this reason, we focused our analysis on both MediaPipe 3D and the marker-based system. We observed that individuals with lower levels of impairment (C7; green markers in Fig. 4) exhibited greater wrist angles and smaller shoulder angles compared to those with more severe impairments (C6: orange markers; C5: red markers, as shown in Fig. 4). Although the methods showed consistent correlations overall, MediaPipe 3D extracted slightly different shoulder angle values for Pose 2 and Pose 3, whereas the marker-based system reported similar values for these poses.

3.3. Trial-by-trial repeatability of pose estimation algorithms in quantifying motion patterns

For all methods, the factor 'repetition' and the interaction term 'repetition * population' were not statistically significant (all $p > 0.8$ across methods). This suggests that the measurements remain consistent across repetitions of the same gesture for both the cSCI and the unimpaired participants. Furthermore, the lack of difference in the pose measures across trials underscored the repeatability, and the reliability, of the markerless approaches. Although repeatability across repetitions was consistently high across methods, differences emerged when comparing the variability of measurements across different poses and algorithms. Overall, simpler configurations such as Pose 1 showed low standard deviations in both the marker-based and markerless systems (Supplementary Table IV), suggesting stable estimation of joint positions in conditions with good joint visibility and limited occlusion. For example, elbow angle and shoulder angle variability in Pose 1 remained in most cases below 1° across all methods, indicating robust detection of extended arm positions. Pose 2 introduced more variability, particularly in shoulder and elbow angle estimation for markerless methods. This pose involves elbow flexion with the hands positioned behind the head, which increases the likelihood of occlusions and complex limb configurations. This determines the difficulty of obtaining trustworthy results in the 2D methods, and standard deviations increased, most notably in MediaPipe 3D. This confirm that 3D models can be sensitive to the biomechanical complexity and self-occlusion introduced by certain postures. Pose 3, involving overhead extension, was less affected, possibly because the extended arms and upright trunk allow better visibility of joints in the frontal plane. Pose 4 showed slightly higher variability in elbow angle estimation across markerless methods compared to Poses 1 and Pose 3. This difference was not statistically significant, and no similar increase was observed in the marker-based system, suggesting that the variability may not reflect true motor instability. Instead, it could be influenced by the specific geometric configuration of the pose, 90° elbow flexion with external rotation, which may amplify the effect of small inaccuracies in keypoint localization, particularly around the elbow. This sensitivity appears more pronounced for the Alphapose 2D method, where the absence of depth information can lead to greater distortion in computed joint angles due to minor out-of-plane movements. A modest level of variability was also noted in MediaPipe 3D, possibly due to challenges in reconstructing joint centers in flexed configurations. These findings suggest that even poses with clear visual exposure can introduce subtle estimation challenges in markerless systems due to a combination of geometric and algorithmic factors. These pose-specific variations in variability highlight that, beyond average repeatability, the stability of joint estimation in markerless systems is influenced by task-specific biomechanical factors and that while markerless methods perform well

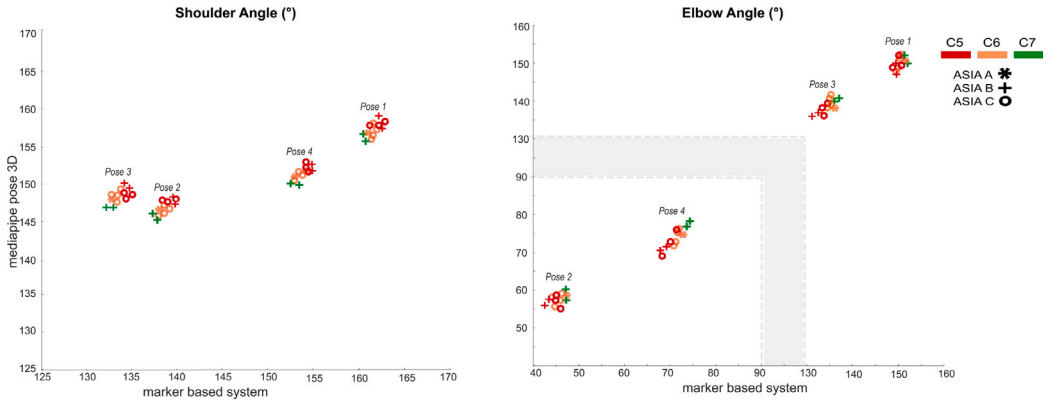

Fig. 4. Shoulder (left) and wrist (right) for the four poses. On the x axis the angles extracted with MediaPipe 3D and on the y axis the angles extracted with the marker-based system. In green, orange and red we highlight individuals with C7, C6 and C5 lesions, respectively. The shape of the marker depends on the ASIA grade. In the elbow angle graph, a gray band indicates an omitted range (90°–130°), which was excluded to improve visualization and focus on the relevant data.

in terms of repeatability under favorable visibility conditions, caution is warranted for poses that involve joint occlusion or close body-limb configurations.

4. Discussion

This study addresses a significant gap in the markerless motion capture analysis for assessing upper limb motor function in individuals with cervical spinal cord injury (cSCI). Although recent advances in video-based human pose estimation have shown considerable promise in clinical applications [52–55], their application to upper limb evaluation in the cSCI population remains limited. Existing studies are often restricted to small cohorts and focus primarily on predictive outcomes or rehabilitation monitoring [56,57], with limited exploration of different pose estimation algorithms or analyses of compensatory movement patterns in relation to lesion severity. To address these limitations, the present work offers a systematic evaluation of three markerless pose estimation algorithms, MediaPipe 2D, AlphaPose, and MediaPipe 3D, compared against a gold-standard marker-based stereophotogrammetric system. Individuals with cSCI and matched unimpaired controls performed standardized bilateral motor tasks from a clinically validated protocol [58]. The results indicate that markerless methods can detect group-level differences in motor performance, with outcomes closely aligned with those of the marker-based system. MediaPipe 3D, in particular, demonstrated greater sensitivity in capturing compensatory strategies associated with more severe impairments. All tested algorithms also showed strong repeatability across trials, supporting their potential for use in both clinical and home-based rehabilitation settings.

4.1. Ability of pose estimation algorithms to differentiate motor activity between SCI and unimpaired populations

To assess the ability of pose estimation algorithms in detecting different motor performance between the two populations, we focused on two parameters: angles and normalized heights. We compared the results obtained from marker-based and markerless approaches to determine if they were consistent in detecting these differences. All methods confirmed the challenges faced by participants with cervical spinal cord injuries (cSCI) compared to unimpaired participants for all the poses. Indeed, significant differences in motor performance were detected by both marker-based and markerless methods, supporting the potential of markerless approaches in detecting neuromotor deficits in real-world clinical settings and, eventually, changes that might occur over time due to the positive effects of rehabilitative treatments or the worsening of the participants' physical conditions. However, the 2D detection algorithm cannot provide a result for Pose 2 due to the occlusion of the wrist keypoints. To address this issue, integrating a 3D pose estimation algorithm proved beneficial, as it could overcome these occlusions and deliver more comprehensive data. Although the MediaPipe 3D algorithm introduced more variability compared to the marker-based system, it was still able to estimate the pose, which makes it a viable and practical alternative. The ability of the 3D algorithm to generate estimates, even when facing occlusions or complex movements, demonstrates its potential for use in scenarios where 2D algorithms fall short. The large effect sizes observed in Pose 2 and Pose 3 (Supplementary Table I) indicate that the differences between the SCI and control groups are not only statistically significant, but also clinically meaningful. Conversely, the small η^2 values observed in Pose 1 and Pose 4 indicate that these configurations may be less informative for distinguishing between populations, potentially due to biomechanical or algorithmic factors rather than sample limitations. In fact, Pose 1 showed only small effects for both joints, which aligns with its lower biomechanical demands and the fact that it was designed to be the least challenging of the four. Pose 4, while intended to be more complex due to the 90° elbow flexion and outward rotation, produced negligible group differences (Supplementary Table I). This observation may be attributed to two factors. First, it could indicate a reduced sensitivity of our kinematic metrics in detecting between-group differences in this specific configuration, potentially due to geometric ambiguities or limitations in joint angle estimation, as elaborated in the revised manuscript. Alternatively, it may reflect a biomechanical pattern: although Pose 4 is among the most challenging, the elbow position remains aligned with the shoulder and does not require additional elevation, unlike in Pose 2 and Pose 3, thus sharing a key characteristic with Pose 1.

4.2. Ability in highlighting motor differences between disability levels

Our findings indicate that differences in motor performance can be distinguished among individuals with varying levels of spinal cord injury (C5, C6, C7), particularly in motor strategies involving the shoulder and wrist. As lesion level increases, a greater ratio between shoulder and elbow movements is observed, reflecting increased reliance on proximal joints due to impaired distal control [62,63]. MediaPipe 3D effectively captured these variations, yielding results consistent with the marker-based system. This demonstrates its potential utility in assessing motor function across varying levels of impairment. In contrast, the 2D methods (MediaPipe 2D and AlphaPose) failed to show a clear relationship between the computed index and lesion level. This may be due to their limited depth perception and reduced accuracy in capturing joint positions during out-of-plane movements or subtle postural adjustments. Although both 2D methods captured the general arm configuration, they lacked the spatial resolution needed to detect compensatory shoulder strategies, particularly in individuals

with higher lesion levels. The compressed distribution of $R_{S,W}$ values in the 2D methods further supports their limited sensitivity, as no consistent trend across lesion levels was observed. This contrasts with the clearer progression seen in both MediaPipe 3D and the marker-based system, where $R_{S,W}$ values systematically increased from C7 to C5, consistent with greater proximal compensation. While MediaPipe 3D showed a significant correlation between the $R_{S,W}$ index and lesion level, some individual discrepancies compared to the marker-based system were noted (Figs. 3 and 4). These may stem from small errors in depth estimation or pose-dependent effects, though likely minimized since most movements occurred within the image plane. Additionally, differences in shoulder angle estimations between the two systems (notably between Poses 2 and 3 in Fig. 4) likely result from how joint positions are defined. The marker-based system uses fixed anatomical landmarks, such as the acromion, while MediaPipe estimates a virtual joint center that may shift with posture or depth inaccuracies, leading to variation in joint position and angle estimation.

4.3. Trial-by-trial repeatability of pose estimation algorithms in quantifying motion patterns

Because of the differences in the parameters' values due to the different placement of virtual markers compared to physical markers, we evaluate the repeatability of the results across repetitions. All methods, MediaPipe 2D, AlphaPose, MediaPipe 3D, and marker-based, did not detect differences across trial repetitions for either the cSCI participants or the control group. This underscores that both marker-based and markerless approaches provide repeatable measures across trials. In other words, this result confirms that markerless systems are repeatable and can provide stable measures. This makes them reliable tools for analyzing differences between groups with varying motor skills.

4.4. Cautionary notes

While the results of this study underscore the potential of markerless motion capture methods in clinical assessments, it is important to highlight the limitations inherent to these approaches. All analyses in this study were based on approximations of joint rather than precise anatomical joints. While the markerless approaches demonstrated their ability to detect differences in motor performance and provide repeatable results, they do not offer the level of accuracy necessary for certain critical clinical decisions. For instance, in scenarios where precise joint angle measurements are required, such as determining whether to proceed with surgical interventions, markerless methods must be applied in combination with biomechanical models [64,65] and their ability to achieve the necessary accuracy should be carefully evaluated. The markerless motion capture process encompasses multiple stages, including video acquisition, biomechanical data extraction, and the classification and interpretation of significant parameters. Each stage introduces potential sources of error, variability, and bias. To ensure reliable performance across diverse environments and populations, further research is needed to refine and optimize these workflows. Critical research is required to inform key design decisions within markerless motion capture workflows. Areas such as standardizing methods for parameter extraction, integrating biomechanical constraints, and effectively managing occlusions or movement variability remain underexplored. Addressing these challenges will be crucial in unlocking the full potential of markerless systems for research and clinical applications [66]. A limitation of the present study is the relatively small and uneven distribution of participants across lesion severity levels, particularly the limited representation in certain subgroups (*e.g.*, only two individuals in the C7 group). This may affect the generalizability and statistical power of subgroup-specific findings. Despite the small numbers, the correlation between $R_{s,w}$ and lesion level was statistically significant and showed consistency across both the marker-based and MediaPipe 3D methods, supporting the plausibility of the observed relationship. Nevertheless, future research with larger and more balanced samples across lesion severity levels is warranted to further validate and extend the current findings. By acknowledging these limitations, we aim to provide a balanced perspective on the use of markerless motion capture approaches. While they offer substantial advantages, such as accessibility and usability, their current capabilities must be interpreted with caution, particularly in contexts demanding high accuracy, precision and interpretability.

5. Conclusions

In conclusion, this study offers valuable insights into the applicability of markerless approaches to assess bilateral upper limb neuromotor deficits in people with cervical spinal cord injury (cSCI). The results highlight several advantages of the markerless approach: it reduces operational bias, preserves the naturalness of movement, reduces costs, and simplifies set-up, making it suitable for non-laboratory environments. Importantly, the markerless analysis allows to effectively distinguish motor patterns between participants with cSCI and those without impairments, particularly in poses where maintaining arm position against gravity was a challenge for the cSCI group. The repeatability in body landmark detection analysis showed that the markerless approaches provide consistent results, comparable to the marker-based gold standard. Although some limitations were observed, such as the inability of the 2D algorithms to detect keypoints under occlusions, the overall repeatability of the markerless algorithms was reasonably comparable to the marker-based gold standard. However, for applications requiring high precision, such as surgical planning or detailed biomechanical assessments, markerless methods may not yet be suitable. Nonetheless, their ability to capture higher-level motor patterns, combined with their ease of use and low setup cost, suggests they could play a valuable role in rehabilitation monitoring and broader clinical assessments.

CRediT authorship contribution statement

Beatrice Lagomarsino: Writing – original draft, Visualization, Methodology, Investigation. **Antonino Massone:** Writing – review & editing, Data curation. **Francesca Odone:** Writing – review & editing, Supervision. **Maura Casadio:** Writing – review & editing, Supervision, Methodology, Investigation, Conceptualization. **Matteo Moro:** Writing – review & editing, Supervision, Methodology, Investigation, Conceptualization.

Funding

This work was funded by the European Union—NextGenerationEU and by the Ministry of University and Research (MUR), National Recovery and Resilience Plan (NRRP), Mission 4, Component 2, Investment 1.5, project "RAISE—Robotics and AI for Socio-economic Empowerment" (#ECS00000035). This work was also partially funded by the Ministry of University and Research, under the grant agreement n. 202275443 W, project VISIONARY (PRIN 2022).

Declaration of competing interest

The authors declare that they have no known competing financial interests or personal relationships that could have appeared to influence the work reported in this paper.

Acknowledgments

The authors thank Amy Bellitto, Luca Losio, Alice De Luca, Camilla Pierella, and Laura Pellegrino for their contribution in data acquisition.

Appendix A. Supplementary data

Supplementary material related to this article can be found online at https://doi.org/10.1016/j.compbiomed.2025.110908.

References

[1] G. Marchesi, G. Ballardini, L. Barone, P. Giannoni, C. Lentino, A.D. Luca, M. Casadio, Modified functional reach test: Upper-body kinematics and muscular activity in chronic stroke survivors, Sensors 22 (2022).

[2] L. Pellegrino, M. Coscia, M. Muller, C. Solaro, M. Casadio, Evaluating upper limb impairments in multiple sclerosis by exposure to different mechanical environments, Sci. Rep. 8 (2018) 2110.

[3] A. Bellitto, A.D. Luca, S. Gamba, L. Losio, A. Massone, M. Casadio, C. Pierella, Clinical, kinematic and muscle assessment of bilateral coordinated upper-limb movements following cervical spinal cord injury, IEEE Trans. Neural Syst. Rehabil. Eng. 31 (2023).

[4] L. Britten, R. Coats, R. Ichiyama, W. Raza, F. Jamil, S. Astill, Bimanual reach to grasp movements after cervical spinal cord injury, PLoS One 12 (2017) e0175457.

[5] L. Britten, R.O. Coats, R.M. Ichiyama, W. Raza, F. Jamil, S.L. Astill, The effect of task symmetry on bimanual reach-to-grasp movements after cervical spinal cord injury, Exp. Brain Res. 236 (2018).

[6] G.J. Snoek, M.J. Ijzerman, H.J. Hermens, D. Maxwell, F. Biering-Sorensen, Survey of the needs of patients with spinal cord injury: Impact and priority for improvement in hand function in tetraplegics, Spinal Cord 42 (2004).

[7] K.D. Anderson, Targeting recovery: Priorities of the spinal cord-injured population, J. Neurotrauma 21 (2004).

[8] L. Pellegrino, M. Coscia, C. Pierella, P. Giannoni, A. Cherif, M. Mugnosso, L. Marinelli, M. Casadio, Effects of hemispheric stroke localization on the reorganization of arm movements within different mechanical environments, Life 11 (2021).

[9] M. Moro, G. Marchesi, F. Odone, M. Casadio, Markerless gait analysis in stroke survivors based on computer vision and deep learning: A pilot study, in: Proceedings of the ACM Symposium on Applied Computing, Association for Computing Machinery, 2020, pp. 2097–2104.

[10] B. Carse, B. Meadows, R. Bowers, P. Rowe, Affordable clinical gait analysis: An assessment of the marker tracking accuracy of a new low-cost optical 3D motion analysis system, Physiother. (United Kingdom) 99 (2013).

[11] S.L. Colyer, M. Evans, D.P. Cosker, A.I. Salo, A review of the evolution of vision-based motion analysis and the integration of advanced computer vision methods towards developing a markerless system, Sport. Med. - Open 4 (2018).

[12] A. Avogaro, F. Cunico, B. Rosenhahn, F. Setti, Markerless human pose estimation for biomedical applications: a survey, Front. Comput. Sci. 5 (2023).

[13] B. Lagomarsino, V. Falzarano, G. Marchesi, T.F. Delitala, F. Odone, M. Casadio, M. Moro, The Role of Depth for Human Motion Assessment with a Single RGB-D Camera: Preliminary Findings, 2024, pp. 436–440.

[14] V. Bazarevsky, I. Grishchenko, K. Raveendran, T. Zhu, F. Zhang, M. Grundmann, BlazePose: On-device Real-time Body Pose tracking.

[15] V. Bazarevsky, I. Grishchenko, Google AI blog: On-device, real-time body pose tracking with MediaPipe BlazePose, Google AI Blog (2020).

[16] H. Xu, E.G. Bazavan, A. Zanfir, W.T. Freeman, R. Sukthankar, C. Sminchisescu, GHUM GHUML: Generative 3D human shape and articulated pose models, in: Proceedings of the IEEE Computer Society Conference on Computer Vision and Pattern Recognition, 2020.

[17] H.S. Fang, J. Li, H. Tang, C. Xu, H. Zhu, Y. Xiu, Y.L. Li, C. Lu, AlphaPose: Whole-body regional multi-person pose estimation and tracking in real-time, IEEE Trans. Pattern Anal. Mach. Intell. 45 (2023).

[18] H. Abbasi, S.R. Mollet, S.A. Williams, L. Lim, M.R. Battin, T.F. Besier, A.J. McMorland, Deep-learning for automated markerless tracking of infants general movements, Int. J. Inf. Technol. (Singapore) 15 (2023).

[19] M. Moro, V.P. Pastore, C. Tacchino, P. Durand, I. Blanchi, P. Moretti, F. Odone, M. Casadio, A markerless pipeline to analyze spontaneous movements of preterm infants, Comput. Methods Programs Biomed. 226 (2022).

[20] P. Beshara, D.B. Anderson, M. Pelletier, W.R. Walsh, The reliability of the microsoft kinect and ambulatory sensor-based motion tracking devices to measure shoulder range-of-motion: A systematic review and meta-analysis, Sensors 21 (2021).

[21] R. Grunert, A. Krause, S. Feig, J. Meixensberger, C. Rotsch, W.G. Drossel, P. Themann, D. Winkler, A technical concept of a computer game for patients with Parkinson's disease - A new form of PC-based physiotherapy, Int. J. Neurosci. 129 (2019).

[22] E.D. Oña, C. Balaguer, R.C.-D.L. Cuerda, S. Collado-Vázquez, A. Jardón, Effectiveness of serious games for leap motion on the functionality of the upper limb in Parkinson's disease: A feasibility study, Comput. Intell. Neurosci. 2018 (2018).

[23] M.A. Boswell, Ł. Kidziński, J.L. Hicks, S.D. Uhlrich, A. Falisse, S.L. Delp, Smartphone videos of the sit-to-stand test predict osteoarthritis and health outcomes in a nationwide study, Npj Digit. Med. 6 (2023).

[24] T.B. de Gusmão Lafayette, V.H. de Lima Kunst, P.V. de Sousa Melo, P. de Oliveira Guedes, J.M.X.N. Teixeira, C.R. de Vasconcelos, V. Teichrieb, A.E.F. da Gama, Validation of angle estimation based on body tracking data from RGB-D and RGB cameras for biomechanical assessment, Sensors 23 (2023).

[25] A. Latreche, R. Kelaiaia, A. Chemori, A. Kerboua, Reliability and validity analysis of MediaPipe-based measurement system for some human rehabilitation motions, Meas.: J. Int. Meas. Confed. 214 (2023).

[26] M. Moro, G. Marchesi, F. Hesse, F. Odone, M. Casadio, Markerless vs. Marker-based gait analysis: A proof of concept study, Sensors 22 (2022).

[27] L. Wade, L. Needham, M. Evans, P. McGuigan, S. Colyer, D. Cosker, J. Bilzon, Examination of 2D frontal and sagittal markerless motion capture: Implications for markerless applications, PLoS One 18 (2023) e0293917.

[28] B. Scott, M. Seyres, F. Philp, E.K. Chadwick, D. Blana, Healthcare applications of single camera markerless motion capture: a scoping review, PeerJ 10 (2022).

[29] G. Amprimo, G. Masi, G. Pettiti, G. Olmo, L. Priano, C. Ferraris, Hand tracking for clinical applications: Validation of the Google MediaPipe Hand (GMH) and the depth-enhanced GMH-D frameworks, Biomed. Signal Process. Control. 96 (2024) 106508.

[30] D.S.B. Kulkarni, A. Kuppelur, A. Shetty, B. Shashank, T. Sangresakoppa, Analysis of physiotherapy practices using deep learning, Int. J. Res. Appl. Sci. Eng. Technol. 12 (2024) 5084–5089.

[31] A. Latreche, R. Kelaiaia, A. Chemori, A. Kerboua, A new home-based upper- and lower-limb telerehabilitation platform with experimental validation, Arab. J. Sci. Eng. 48 (2023) 10825–10840.

[32] C. Mennella, U. Maniscalco, G.D. Pietro, M. Esposito, A deep learning system to monitor and assess rehabilitation exercises in home-based remote and unsupervised conditions, Comput. Biol. Med. 166 (2023) 107485.

[33] B. Pereira, B. Cunha, P. Viana, M. Lopes, A. Melo, A. Sousa, A machine learning app for monitoring physical therapy at home, Sensors 24 (2023) 158.

[34] A.D. Miguel-Rubio, M.D. Rubio, A. Salazar, J.A. Moral-Munoz, F. Requena, R. Camacho, D. Lucena-Anton, Is virtual reality effective for balance recovery in patients with spinal cord injury? A systematic review and meta-analysis, J. Clin. Med. 9 (2020).

[35] J. Adolf, P. Kán, T. Feuchtner, B. Adolfová, J. Doležal, L. Lhotská, Offistretch: camera-based real-time feedback for daily stretching exercises, Vis. Comput. 41 (2025) 1555–1571.

[36] S. He, D. Meng, M. Wei, H. Guo, G. Yang, Z. Wang, Proposal and validation of a new approach in tele-rehabilitation with 3D human posture estimation: a randomized controlled trial in older individuals with sarcopenia, BMC Geriatr. 24 (2024) 586.

[37] M. Petracca, N. Petsas, G. Sellitto, I. Ruotolo, C. Livi, V. Bonanno, F. Felicetti, A. Ianniello, S. Ruggieri, G. Borriello, C. Pozzilli, Telerehabilitation and onsite rehabilitation effectively improve quality of life, fatigue, balance, and cognition in people with multiple sclerosis: an interventional study, Front. Neurol. 15 (2024).

[38] A. Arntz, F. Weber, M. Handgraaf, K. Lällä, K. Korniloff, K.P. Murtonen, J. Chichaeva, A. Kidritsch, M. Heller, E. Sakellari, C. Athanasopoulou, A. Lagiou, I. Tzonichaki, I. Salinas, P. Martínez-Bueso, O. Velasco-Roldán, R.J. Schulz, C. Grüneberg, Technologies in home-based digital rehabilitation: Scoping review, JMIR Rehabil. Assist. Technol. 10 (2023).

[39] V. Cimolin, L. Vismara, C. Ferraris, G. Amprimo, G. Pettiti, R. Lopez, M. Galli, R. Cremascoli, S. Sinagra, A. Mauro, L. Priano, Computation of gait parameters in post stroke and Parkinson's disease: A comparative study using RGB-D sensors and optoelectronic systems, Sensors 22 (2022).

[40] R. Kaur, R.W. Motl, R. Sowers, M.E. Hernandez, A vision-based framework for predicting multiple sclerosis and Parkinson's disease gait dysfunctions - A deep learning approach, IEEE J. Biomed. Heal. Inform. 27 (2023).

[41] T. Khan, A. Zeeshan, M. Dougherty, A novel method for automatic classification of Parkinson gait severity using front-view video analysis, Technol. Health Care 29 (2021).

[42] T. Li, J. Chen, C. Hu, Y. Ma, Z. Wu, W. Wan, Y. Huang, F. Jia, C. Gong, S. Wan, L. Li, Automatic timed up-and-go sub-task segmentation for Parkinson's disease patients using video-based activity classification, IEEE Trans. Neural Syst. Rehabil. Eng. 26 (2018).

[43] L. Lonini, Y. Moon, K. Embry, R.J. Cotton, K. McKenzie, S. Jenz, A. Jayaraman, Video-based pose estimation for gait analysis in stroke survivors during clinical assessments: A proof-of-concept study, Digit. Biomarkers 6 (2022).

[44] S. Mehdizadeh, A. Sabo, K.D. Ng, A. Mansfield, A.J. Flint, B. Taati, A. Iaboni, Predicting short-term risk of falls in a high-risk group with dementia, J. Am. Med. Dir. Assoc. 22 (2021).

[45] B. Muñoz-Ospina, D. Alvarez-Garcia, H.J.C. Clavijo-Moran, J.A. Valderrama-Chaparro, M. García-Peña, C.A. Herrán, C.C. Urcuqui, A. Navarro-Cadavid, J. Orozco, Machine learning classifiers to evaluate data from gait analysis with depth cameras in patients with Parkinson's disease, Front. Hum. Neurosci. 16 (2022).

[46] K.D. Ng, S. Mehdizadeh, A. Iaboni, A. Mansfield, A. Flint, B. Taati, Measuring gait variables using computer vision to assess mobility and fall risk in older adults with dementia, IEEE J. Transl. Eng. Heal. Med. 8 (2020).

[47] B.M. Ospina, J.A.V. Chaparro, J.D.A. Paredes, Y.J.C. Pino, A. Navarro, J.L. Orozco, Objective arm swing analysis in early-stage Parkinson's disease using an RGB-D Camera (Kinect®), J. Parkinson's Dis. 8 (2018).

[48] A. Procházka, O. Vyšata, M. Vališ, O. Ťupa, M. Schätz, V. Mařík, Use of the image and depth sensors of the Microsoft Kinect for the detection of gait disorders, Neural Comput. Appl. 26 (2015).
[49] J.H. Shin, R. Yu, J.N. Ong, C.Y. Lee, S.H. Jeon, H. Park, H.J. Kim, J. Lee, B. Jeon, Quantitative gait analysis using a pose-estimation algorithm with a single 2D-video of Parkinson's disease patients, J. Parkinson' s Dis. 11 (2021).
[50] G. Morinan, Y. Peng, S. Rupprechter, R.S. Weil, L.A. Leyland, T. Foltynie, K. Sibley, F. Baig, F. Morgante, R. Gilron, R. Wilt, P. Starr, J. O'Keeffe, Computer-vision based method for quantifying rising from chair in Parkinson's disease patients, Intelligence- Based Med. 6 (2022).
[51] M. Moro, G. Marchesi, M. Cellerino, G. Boffa, F. Odone, M. Inglese, M. Casadio, Markerless video-based gait analysis in people with multiple sclerosis, IEEE Trans. Neural Syst. Rehabil. Eng. (2025).
[52] P. Jayavel, H.K. Srinivasan, V. Karthik, A. Fouly, A. Devaraj, Human upper limb kinematics using a novel algorithm in post-stroke patients, Proc. Inst. Mech. Eng. Part H: J. Eng. Med. 239 (2025) 48–55.
[53] W.W. Lam, K.N. Fong, C.-W. Chien, Upper limb kinematic measurement using markerless motion capturing (MMC) in stroke survivors: A cross-sectional experimental study, DIGITAL HEALTH 11 (2025).
[54] S. Baker, A. Tekriwal, G. Felsen, E. Christensen, L. Hirt, S.G. Ojemann, D.R. Kramer, D.S. Kern, J.A. Thompson, Automatic extraction of upper-limb kinematic activity using deep learning-based markerless tracking during deep brain stimulation implantation for Parkinson's disease: A proof of concept study, PLoS ONE 17 (2022).
[55] A. Bandini, S. Orlandi, F. Giovannelli, A. Felici, M. Cincotta, D. Clemente, P. Vanni, G. Zaccara, C. Manfredi, Markerless analysis of articulatory movements in patients with Parkinson's disease, J. Voice 30 (2016) 766.e1–766.e11.
[56] H.J. Lee, S.M. Jin, S.J. Kim, J.H. Kim, H. Kim, E.K. Bae, S.K. Yoo, J.H. Kim, Development and validation of an artificial intelligence-based motion analysis system for upper extremity rehabilitation exercises in patients with spinal cord injury: A randomized controlled trial, Heal. (Switzerland) 12 (2024).
[57] M. Narendra, P. Mohanty, L.J. Anbarasi, V. Ravi, Virtual analysis for spinal cord injury rehabilitation, Open Biomed. Eng. J. 18 (2024).
[58] M. I. Classification, VLT.
[59] R.B. Davis, S. Õunpuu, D. Tyburski, J.R. Gage, A gait analysis data collection and reduction technique, Hum. Mov. Sci. 10 (1991).
[60] F.N. Fritsch, R.E. Carlson, Monotone piecewise cubic interpolation, SIAM J. Numer. Anal. 17 (1980).
[61] M.W. Whittle, Gait Analysis: An Introduction, fifth ed., Butterworth-Heinemann, Oxford, UK, 2014.
[62] S. Mateo, A. Roby-Brami, K.T. Reilly, Y. Rossetti, C. Collet, G. Rode, Upper limb kinematics after cervical spinal cord injury: A review, J. NeuroEng. Rehabil. 12 (2015).
[63] J.Y. Gefen, A.S. Gelmann, G.J. Herbison, M.E. Cohen, R.R. Schmidt, Use of shoulder flexors to achieve isometric elbow extension in C6 tetraplegic patients during weight shift, Spinal Cord 35 (1997).
[64] S.D. Uhlrich, A. Falisse, Ł. Kidziński, J. Muccini, M. Ko, A.S. Chaudhari, J.L. Hicks, S.L. Delp, OpenCap: Human movement dynamics from smartphone videos, PLoS Comput. Biol. 19 (2023).
[65] R. Yang, A. Kennedy, R.J. Cotton, BiomechGPT: Towards a biomechanically fluent multimodal foundation model for clinically relevant motion tasks, 2025.
[66] R.J. Cotton, PosePipe: Open-source human pose estimation pipeline for rehabilitation research, Arch. Phys. Med. Rehabil. (2022).